



A terahertz dual-band metamaterial perfect absorber based on metal-dielectric-metal multi-layer columns

Pouria Zamzam¹ · Pejman Rezaei¹

Received: 11 September 2020 / Accepted: 28 January 2021 / Published online: 9 February 2021
© The Author(s), under exclusive licence to Springer Science+Business Media, LLC part of Springer Nature 2021

Abstract

In this paper, a new model of multi-layer metamaterial perfect absorber (MPA) in the terahertz region has been introduced. This model is similar to the classic absorber model, ie the three traditional layers of metal-dielectric-metal. The difference is that the middle layer has changed in height and consists of 3 separate layers with the same material. Therefore, the middle layer of the proposed structure is metamaterial. Numerical results of the simulation show that the absorption rate of the perfect absorber at 6.86 THz is 99.99%. Also, by changing the width of the two middle layer columns w , a dual-band perfect absorber with an average absorption rate of 97.18% is obtained at frequencies of 4.24 THz and 6.86 THz. A significant advantage of this paper over other works is that this absorber is adjustable, in addition to obtaining a nearly perfect dual-band absorber with a narrow-band peak by adjusting the parameters and also a nearly broad-band absorber can also be obtained by changing the parameters without re-manufacturing the structure. We believe that the proposed absorber has potential in filtering, detection and imaging.

Keywords Metamaterial · Perfect absorber · Terahertz · Dual-band · Tunable

1 Introduction

Metamaterials (MMs) are engineered materials and their properties are often not found in nature, for example: negative refractive index, cloaking behavior, negative permittivity, invisibility, reverse doppler effects and perfect absorption. Today MMs have expanded into high frequency domains such as microwave (Smith et al. 2000), mm-wave (Gokkavas et al. 2006), THz (Yen et al. 2004), infrared and optics (Pereira and Shulika 2011; Choi 2015). These materials derive their properties from their structure and not just from their composition. For the first time, Veselago offered a theory about material with a negative refractive index (simultaneously ϵ and μ are negative) (Veselago 1968). All materials affect electromagnetic waves through two properties of permittivity coefficient and permeability coefficient. Metamaterials are also introduced by complex electric permittivity ($\epsilon(\omega) = \epsilon_1 + j\epsilon_2$) and complex magnetic permeability ($\mu(\omega) = \mu_1 + j\mu_2$). Most researchers focus on the real

✉ Pejman Rezaei
prezaei@semnan.ac.ir

¹ Semnan University, Semnan, Islamic Republic of Iran

part ϵ and μ to achieve a negative refractive index and try to minimize the imaginary part ϵ and μ to reduce losses, but these imaginary parts have a great effect on some strange and unique properties of MMs. one of which is the property of absorbing electromagnetic waves. Therefore, MM can be used in terahertz absorber structures. Absorbers are structures through which electromagnetic energy is not reflected and not transmitted. The use of MM with metal creates a very strong perfect absorption structure. So, metamaterial perfect absorber (MPA) is an attractive branch in the terahertz frequency.

The classic and traditional form of MPA structures is that three layers of metal-dielectric-metal are formed so that the middle layer, which is made of a dielectric, is sandwiched between two strong conductive layers such as gold.

The advantage of having a high conductive layer on the top of the structure is that by matching the impedance to air, reflection can be eliminated. If a percentage of the EM wave passes through the top layer, it is wasted in the middle layer due to the middle layer's loss. The third or bottom layer, called the ground Prevents any waves from passing through the structure. Therefore, perfect absorption can be achieved. Many kinds of MPAs such as single-band (Faruk and Sabah 2019; Ebrahimi 2020; Luo and Cheng 2020), dual-band (Xiao et al. 2018; Li and Cheng 2020), multi-band (wang et al. 2014; Hu et al. 2016; Wang and Wang 2016; Meng et al. 2018) and broad-band (Zhu et al. 2014; Jindal and kumal 2015; Arik et al. 2017; Tang et al. 2017; Barzegar-Parizi 2018; Dong and Chen 2018; Soheilifar 2018; Patel et al. 2020a, b) and also MPA based on graphene metasurface in terahertz region (He et al. 2015; Xiao et al. 2017; Ye et al. 2017; Huang et al. 2018; Zhang et al. 2018; Barzegar-Parizi 2019; Daraei et al. 2020; Mishra and Panwar 2020) and micro-wave region (Ghods and Rezaei 2018) has been introduced.

In this paper, a new classical MPA model with three layers (metal-dielectric-metal) but with a change in the height of the middle layer is introduced as a unit cell. In the discussion of filters, we use the phrase of MIM (metal-insulation-metal) (Khani et al. 2019a, b; Khani et al. 2019a, b). Numerical results show that a single-band with an absorption of 99.99% and also a dual-band with an average absorption of 97.18% is obtained. So, we have a single-band perfect absorption and a dual-band nearly perfect absorption with only one structure. Another advantage of this structure is that it is adjustable, ie by changing and optimizing the effective parameters, a nearly narrow peak or a nearly wide peak is obtained. The great advantage of this absorber is that all of these results are achieved without re-manufacturing the structure but also by changing the effective parameters. Based on the finite-difference time domain (FDTD) method, the proposed absorber in this paper was calculated and optimized numerically. In all simulation periodic boundary conditions were set in the x-and y-axis and perfectly matched layer boundary condition was used along z-axis. Here it is assumed that the source was the plane wave, which was normally incident onto the structure.

2 Structure design and simulation

Figure 1 shows a schematic of the absorber unit cell suggested in this paper. As can be seen in the Fig. 1, it is obvious that the structure consists of 3 layers. A perfect conductor (gold) with a thickness of $0.2 \mu\text{m}$ and with a conductivity of $\sigma = 2.2 \times 10^5 \text{S/m}$ is used for the top and bottom of the structure. The middle layer SiO_2 consists of a dielectric with a constant of $\epsilon = (2.79 + j0.31)$ and thicknesses of m and $h1$. The presence of a perfect conductor (gold) on the bottom of the structure is because no waves pass through the structure

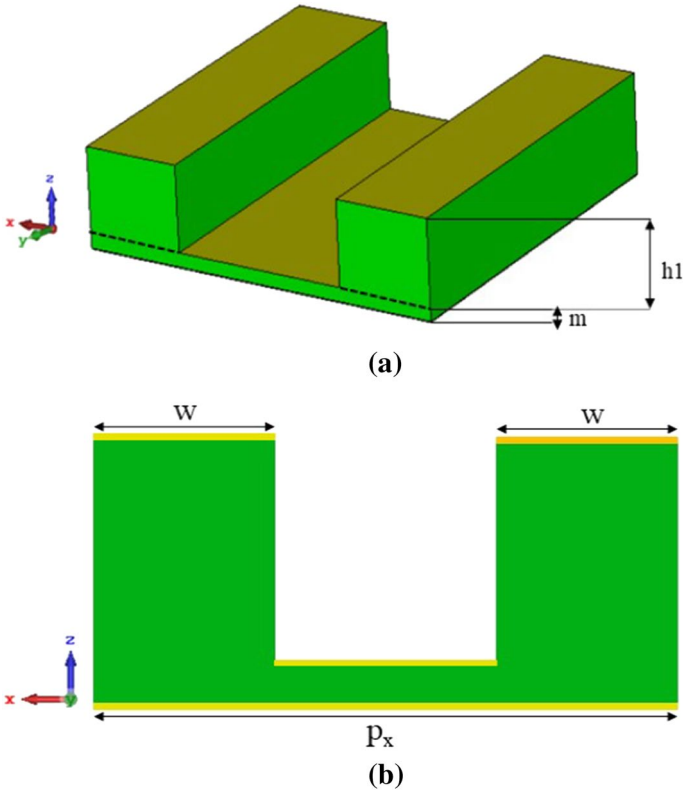


Fig. 1 The schematics of a single unit cell. **a** Perspective view. **b** Side view. ($w=25 \mu\text{m}$, $m=3.5 \mu\text{m}$, $h1=19.5 \mu\text{m}$, $p_x=p_y=9 \mu\text{m}$)

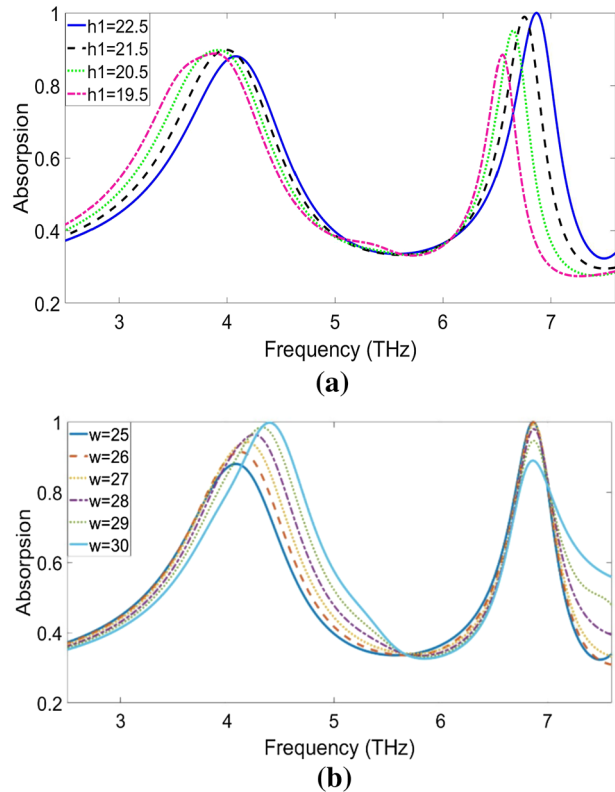
because the thickness of this bottom layer ($0.2 \mu\text{m}$) is bigger than typical skin depth in the THz range. The absorptivity of the presented metamaterial absorber can be defined as $A=1-T-R$ where T is transmissivity and R is reflectivity (Wang et al. 2015). Due to the reason stated above, $T=0$, then the absorption can be obtained by $A=1-R$. Hence the bottom layer is also called the mirror. So A (absorption) can get very close to 1 when the reflection is close to zero ($R=0$, impedance ($z=1$) matched to the free space).

Our results are obtained through the period structures are illuminated by a normally incident plane wave and perfectly matched layers (PML) are applied along the z direction and period boundary conditions in the x and y directions.

3 Results and discussion

As shown in Fig. 2, the effects of changes in the height and width of the middle layer column (w , $h1$) on the absorption intensity are very noticeable. The basis of our discussion in this article is a normal incidence wave. In Fig. 2a, when the height of the middle layer columns is $h1=22.5 \mu\text{m}$, the structure has two absorption peaks of 88.81% and 88.45% at 3.88 THz and 6.54 THz, respectively. In this case, with the reduction of $h1$

Fig. 2 Absorption spectra of the presented MPA; **a** with different column height (h_1), **b** with different column width (w)



from 22.5 to 19.5 μm , the intensity of peak absorption will reach 88.03% and 99.99% at frequencies of 4.08 THz and 6.86 THz, respectively. So, a dual-band absorber with an average absorption of 94.01% is obtained.

Moreover, according to Fig. 2b, as the width of the columns increases from 25 to 30 μm , the low frequency absorption intensity increases and the high frequency absorption intensity decreases. Thus that, when $w = 25 \mu\text{m}$, one of the absorption peaks is 99.99% at the high frequency of 6.86 THz and the absorption intensity of the second peak is 88.03% at the low frequency of 4.08 THz and when $w = 30 \mu\text{m}$ higher absorption intensity occur at a lower frequency and lower absorption intensity occur at a higher frequency, ie the structure has two absorption peaks of 99.79% and 88.99% at 4.93 THz and 6.85 THz frequencies, respectively. But the best possible case is when $w = 28 \mu\text{m}$. Because in this case, a dual-band nearly perfect absorber with an average absorption of 97.18% at frequencies of 4.24 THz and 6.86 THz is obtained.

We will now see why the effects of changing the above parameters affect the intensity of absorption. As seen and discussed in Fig. 2, it is obvious that changes in the height of h_1 have a direct effect on the absorption intensity of the second peak (higher frequency). By increasing the h_1 thickness from 19.5 to 22.5 μm , the first peak (lower frequency) remains almost constant, but the second peak reaches the best state, ie 99.99% absorption. The reason for this phenomenon is that when the thickness of the dielectric is small, the interaction between two metal layers is very strong (top and bottom layers). Therefore, as this thickness increases, the interaction between these two layers becomes

Fig. 3 Absorption spectra of the presented MPA with various in (m1) heights

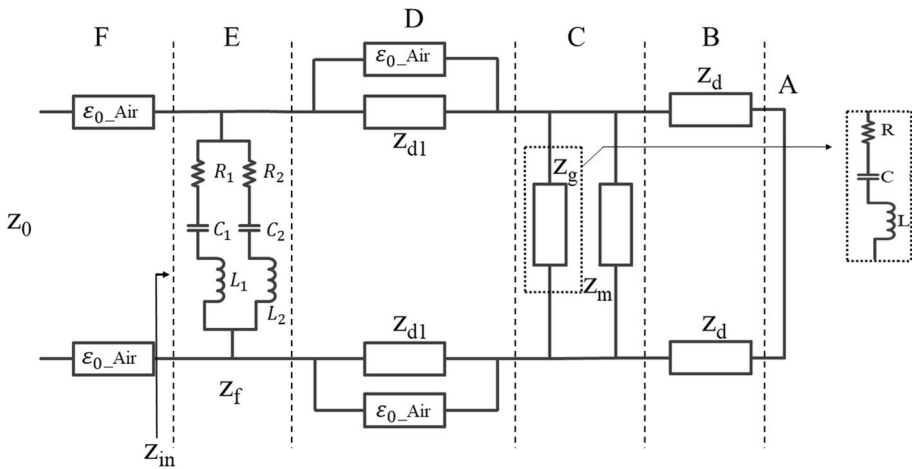
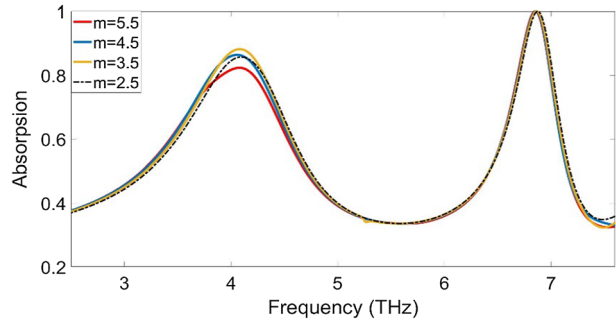


Fig. 4 Equivalent circuit model of proposed PMA

weak. So the thickness of h_1 has a significant influence on absorption intensity of the second peak.

The effect of m height changes on the first peak is also investigated (when $u = 2 \mu\text{m}$ and $h = 19.5 \mu\text{m}$). As can be seen in Fig. 3, when $m = 5.5 \mu\text{m}$ the first peak has an absorption of 82.29% at a frequency of 4.07 THz and the second peak has an absorption of 99.99% at a frequency of 6.85 THz. Then, with a decrease of (m) from 5.5 to 3.5 μm , the first peak remains at the same frequency has an absorption of 88.03% (at the frequency of 4.07 THz) and the second peak with the same absorption (99.99%) at the same frequency (6.85 THz).

4 Equivalent circuit modeling

We use the transmission line mode to analyze the equivalent circuit model of the reported PMA unit, as shown in Fig. 4. These absorption intensity changes can be understood according to the circuit model of the proposed structure. As you can see in Fig. 4, We divided the equivalent circuit into six parts for further investigation from A to F. According to Equation $A(\omega) = 1 - T(\omega) - R(\omega)$, due to the strong conductivity of the bottom layer, $T(\omega)$ becomes zero. So part A is the metal Gold plane at the bottom, which acts as a short

circuit. Part B is a dielectric layer transmission line model that depends on the height m . Part C consists of two parallel impedances of z_m and z_g . The impedance z_m is shown with the gold_dielectric interference impedance. z_g is also considered as the only gold impedance. Part D consists of two parallel parts z_{d1} and the spacing between two dielectric columns, which depends on the height $h1$. Part E consists of two RLC circuits connected parallel corresponding to the top (gold) structure. Finally, Part A is a free space transmission line with characteristic impedance Z_0 .

The absorption of the proposed absorber can be obtained from:

$$A(\omega) = 1 - \left| \frac{z_{in}(\omega) - z_0}{z_{in}(\omega) + z_0} \right| \tag{1}$$

Z_{in} is the input impedance of the PMA, expressed as:

$$Z_{in}(\omega) = \frac{1}{z_f(\omega)} + \frac{1}{z_{d1}(\omega)||z_0} + \frac{1}{z_g(\omega)} + \frac{1}{z_m(\omega)} + \frac{1}{z_d(\omega)} \tag{2}$$

Here in:

$$z_f(\omega) = \frac{1}{R_1 + j\omega L_1 + \frac{1}{j\omega C_1}} + \frac{1}{R_2 + j\omega L_2 + \frac{1}{j\omega C_2}} \tag{3}$$

$$z_{d1}(\omega) = j\sqrt{\frac{\omega_r \omega_0}{\epsilon_r \epsilon_0}} \cdot \tan(kd_1) \tag{4}$$

$$z_g = \frac{1}{\sigma_g} \tag{5}$$

$$z_m = \frac{z_{d1}(\omega)}{\frac{2\sqrt{n_1 n_2}}{T} - (n_1 + n_2)} \tag{6}$$

$$z_d(\omega) = j\sqrt{\frac{\omega_r \omega_0}{\epsilon_r \epsilon_0}} \cdot \tan(kd) \tag{7}$$

$$k = \frac{k_0}{\sqrt{\epsilon_r k_r}} \tag{8}$$

where k , ω_r , ϵ_r , are wavenumber, permeability, and relative permittivity of the SiO₂ dielectric layer, and k_0 , ω_r , ϵ_r are wavenumber, permeability, and relative permittivity of the free space, respectively. Also, n_1 and n_2 are the refractive indexes of dielectric and gold material and Z_0 is air impedance ($\sim 377 \Omega$). d and d_1 also correspond to the metamaterial heights shown in Fig. 1. When $Z_{in}(\omega) = Z_0$, PMA can achieve perfect absorption (Patel et al. 2020a, b). Then by changing the geometric parameters of structure can vary the input impedance of PMA.

In order to better justify the absorption mechanism of the proposed structure, the distribution of the electric field in the two absorption frequencies is shown in Fig. 5. As shown

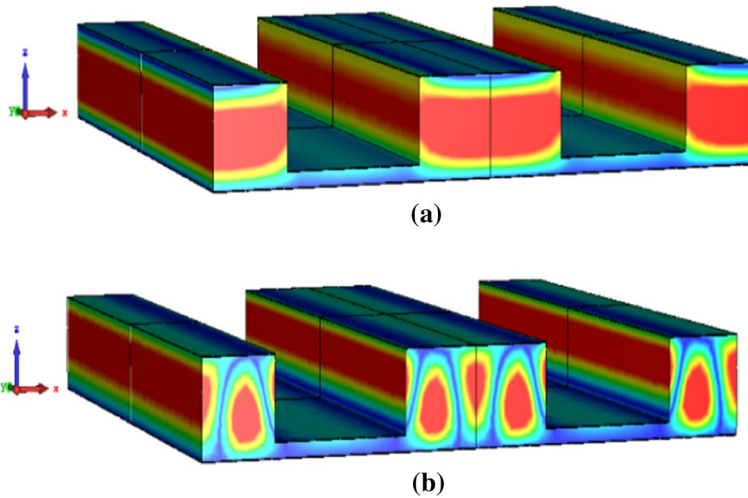


Fig. 5 Simulated unit cell perspective view distributions of the electric field at two frequencies. **a** 4.39 THz (first peak); **b** 6.86 THz (second peak)

in Fig. 5 (a), at the first peak (4.39 THz) most transient wave losses occur in the center strip of the middle layer columns. In fact, above the height of m , the two columns together with the air distance between the two columns are a combination of 2 dielectrics, which when we increase the width of these columns w due to the stronger and higher constant dielectric of this combination and smaller distance of air, the absorption rate of the first peak is much higher. In Fig. 5 (b) most of the electric field is concentrated in the center and sides of the two columns of the dielectric layer, and most of the losses occur in the air space between the two columns, which was observed that the absorption intensity of the second peak decreases significantly with increasing width w .

Table 1 tries to compare the work of this article with several other articles in terms of average absorption and it is observed that in 2 frequencies of 4.24 THz and 6.86 THz, the average absorption reached 97.18% which is better than other works in the table.

As can be seen from Table 1, the proposed article has been compared with several other articles. The main advantage of the proposed paper over other papers is in the results. We

Table 1 Comparison of the proposed absorber with the reported state-of-the-art

Ref	Peak frequencies (THz)	Peak numbers	Average absorption
Arezoomand et al. (2015)	0.53, 0.84, 0.98	3	92.73%
Chen and Fan (2015)	0.72, 1.4, 2.3	3	90.66%
Shan et al. (2015)	0.41, 0.75	2	94.8%
Wang et al. (2015)	1.46, 2.89	2	94.11%
Liu et al. (2016)	0.55, 1.6	2	> 95%
Huang et al. (2018)	0.85, 3.37	2	95.15%
Mohanty et al. (2018)	1.45, 1.8, 2.7, 3.1, 3.7	5	80.244
Appasani et al. (2019)	1.05, 2.16, 3.59, 3.87	4	95.34%
Proposed	4.24, 6.86	2	97.18%

obtained higher absorption peaks at different frequencies. The proposed article has an average absorption of 97.13%, which has a higher absorption percentage than other articles.

5 Conclusion

As a conclude, a novel nearly perfect and adjustable dual-band absorber is introduced. This structure is the same as the classical and traditional structure of adsorbents, ie metal-dielectric-metal, with the difference that the dielectric layer of the adsorbent proposed in this article has a change in height or in other words, multiple layers. A continuous dielectric layer with height m and then two dielectric columns of the same material is placed on the top of height m . The height m on the first peak or lower frequency and also the height of these columns h_1 on the second peak or higher frequency is very effective. Then by optimizing this value, we will reach a dual-band nearly perfect absorber with absorption of 97.18% at 4.24 THz and 6.86 THz. Finally, the electric field distribution of this structure at two peak frequencies was investigated. This nearly perfect and tunable terahertz absorber has potential in filtering, detection and imaging.

Acknowledgements The authors acknowledge the Semnan University staff for their beneficial and professional help. The authors would like to thank the journal editor and reviewers for their valuable comments.

References

- Appasani, B., Prince, P., Ranjan, R.K., Gupta, N., Verma, V.K.: A simple multi-band metamaterial absorber with combined polarization sensitive and polarization insensitive characteristics for terahertz applications. *Plasmonics* **14**, 737–742 (2019)
- Arezoomand, A.S., Zarrabi, F.B., Heydari, S., Gandgi, N.P.: Independent polarization and multi-band THz absorber base on Jerusalem cross. *Opt. Commun.* **352**, 121–126 (2015)
- Arik, K., AbdollahRamezani, S., Khavasi, A.: Polarization insensitive and broadband terahertz absorber using graphene disks. *Opt. Quant. Electron.* **12**, 393–398 (2017)
- Barzegar-Parizi, S.: Realization of wide-angle and wideband absorber using metallic and graphene-based meta-surface for mid-infrared and low THz frequency. *Opt. Quant. Electron.* **50**, 378 (2018)
- Barzegar-Parizi, S.: Graphene-based tunable dual-band absorbers by ribbon/ disk array. *Opt. Quant. Electron.* **51**, 167 (2019)
- Chen, Z., Fan, W.: Ultra-flexible polarization-insensitive multiband terahertz metamaterial absorber. *Appl. Opt.* **54**, 2376–2382 (2015)
- Choi, J.H.: High-speed devices and circuits with THz applications. CRC Press, Boca Raton (2015)
- Daraei, O.M., Goudarzi, K., Bemani, M.: A tunable ultra-broadband terahertz absorber based on two layers of graphene ribbons. *Opt. Laser Technol.* **122**, 105853 (2020)
- Dong, X., Chen, L.: Ultrabroadband plasmonic absorber based on biomimetic compound eye structures. *IEEE Photon. J.* **10**(1), 5700207 (2018)
- Ebrahimi, S.: Optical absorber based on self-similar cylindrical element for detecting optical material. *Opt. Quant. Electron.* **52**, 87 (2020)
- Faruk, A., Sabah, C.: Absorber and sensor applications of complimentary H-shaped fishnet metamaterial for sub-terahertz frequency region. *Optik* **177**, 64–70 (2019)
- Ghods, M.M., Rezaei, P.: Ultra-wideband microwave absorber based on uncharged graphene layers. *J. Electromag. Waves Appl.* **32**(15), 1950–1960 (2018)
- Gokkavas, M., Guven, K., Bulu, I., Aydin, K., Penciu, R.S., Kafesaki, M., Soukoulis, C.M., Ozbay, E.: Experimental demonstration of a left-handed metamaterial operating at 100 GHz. *Phys. Rev. B* **73**(19), 193103 (2006)
- He, X.J., Yan, S.T., Ma, Q.X., Zhang, Q.F., Jia, P., Wu, F.M., Jiang, J.X.: Broadband and polarization-insensitive terahertz absorber based on multilayer metamaterials. *Opt. Commun.* **340**, 44–49 (2015)
- Hu, D., Wang, H.Y., Zhu, Q.F.: Design of six-band terahertz perfect absorber using a simple U-shaped closed-ring resonator. *IEEE Photon. J.* **8**(2), 1–8 (2016)

- Huang, M., Cheng, Y., Cheng, Z., Chen, H., Mao, X., Gong, R.: Based on graphene tunable dual-band terahertz metamaterial absorber with wide-angle. *Opt. Commun.* **415**, 194–201 (2018)
- Jindal, S., Kumar, M.: Broadband and polarization insensitive design of terahertz absorber with high-index contrast grating on SOI chip. *Opt. Quant. Electron.* **47**, 1693–1702 (2015)
- Khani, S., Danaie, M., Rezaei, P.: Size reduction of MIM surface plasmon based optical bandpass filters by the introduction of arrays of silver nano-rods. *Phys. E Low-Dimens. Syst. Nanostruct.* **113**, 25–34 (2019a)
- Khani, S., Danaie, M., Rezaei, P.: Tunable single-mode bandpass filter based on metal-insulator-metal plasmonic coupled U-shaped cavities. *IET Optoelectron.* **13**(4), 161–171 (2019b)
- Li, W., Cheng, Y.: Dual-band tunable terahertz perfect metamaterial absorber based on strontium titanate (STO) resonator structure. *Opt. Commun.* **462**, 125265 (2020)
- Liu, J., Fan, L., Ku, J., Mao, L.: Absorber: a novel terahertz sensor in the application of substance identification. *Optic. Quant. Electron.* **48**(2), 80 (2016)
- Luo, H., Cheng, Y.: Thermally tunable terahertz metasurface absorber based on all dielectric indium antimonide resonator structure. *Opt. Mater.* **102**, 109801 (2020)
- Meng, T., Hu, D., Zhu, Q.: Design of a five-band terahertz perfect metamaterial absorber using two resonators. *Opt. Commun.* **415**, 151–155 (2018)
- Mishra, R., Panwar, R.: Investigation of graphene fractal frequency selective surface loaded terahertz absorber. *Opt. Quant. Electron.* **52**, 317 (2020)
- Mohanty, A., Acharya, O.P., Appasani, B., Mohapatra, S.K.: A multi-band terahertz metamaterial absorber based on a Π and Ushaped structure. *Photon. Nanostruct.* **32**, 74–80 (2018)
- Patel, S.K., Charola, S., Parmar, J., Ladumor, M., Ngo, Q.M., Dhasarathan, V.: Broadband and efficient graphene solar absorber using periodical array of C-shaped metasurface. *Opt. Quant. Electron.* **52**, 250 (2020a)
- Patel, S.K., Sorathiya, V., Lavadiya, S., Thomas, L., Nguyen, T.K., Dhasarathan, V.: Multi-layered graphene silica-based tunable absorber for infrared wavelength based on circuit theory approach. *Plasmonics* **15**, 1767–1779 (2020b)
- Pereira, M.F., Shulika, O.: Terahertz and mid infrared radiation: generation, detection and applications. Springer, Netherlands (2011)
- Shan, Y., Chen, L., Shi, C., Cheng, Z., Zang, X., Xu, B., Zhu, Y.: ultratin flexible dual band terahertz absorber. *Opt. Commun.* **350**, 63–70 (2015)
- Smith, D.R., et al.: Composite medium with simultaneously negative permeability and permittivity. *Phys. Rev. Lett.* **84**(18), 4184–4187 (2000)
- Soheilifar, M.R.: Wideband optical absorber based on plasmonic metamaterial cross structure. *Opt. Quant. Electron.* **50**, 442 (2018)
- Tang, B., Zhu, Y., Zhou, X., Huang, L., Lang, X.: Wide-angle polarization-independent broadband absorbers based on concentric multisplit ring arrays. *IEEE Photon. J.* **9**(6), 4502707 (2017)
- Vesalago, V.G.: The electrodynamics of substances with simultaneously negative values of ϵ and μ . *Sov. Phys. Usp.* **10**, 509–514 (1968)
- Wang, B.X., Wang, G.Z.: Quad-band terahertz absorber based on a simple design of metamaterial resonator. *IEEE Photon. J.* **8**(6), 1–8 (2016)
- Wang, B.X., Zhai, X., Wang, G.Z., Huang, W.Q., Wang, L.L.: Design of a four-band and polarization insensitive terahertz metamaterial absorber. *IEEE Photon.* **7**(1), 4600108 (2014)
- Wang, B.X., Zhai, X., Wang, G.Z., Huang, W.Q., Wang, L.L.: A novel dual-band terahertz metamaterial absorber for a sensor application. *J. Appl. Phys.* **117**(1), 014504 (2015)
- Xiao, B., Gu, M., Qin, K., Xiao, S.: Absorption enhancement in graphene with an efficient resonator. *Opt. Quant. Electron.* **49**, 177 (2017)
- Xiao, B., Lin, H., Xiao, L., Gu, M., Yang, D., Hu, L., Guo, F., Mi, H.: A tunable dual-band THz absorber based on graphene sheet and ribbons. *Opt. Quant. Electron.* **50**, 370 (2018)
- Ye, L., Chen, Y., Cai, G., Liu, N., Zhu, J., Song, Z., Liu, Q.H.: Broadband absorber with periodically sinusoidally-patterned graphene layer in terahertz range. *Optic. Express.* **25**(10), 11223–11232 (2017)
- Yen, T.J., Padilla, W.J., Fang, N., Vier, D.C., Smith, D.R., Pendry, J.B., Basov, D.N., Zhang, X.: Terahertz magnetic response from artificial materials. *Science.* **303**(5663), 1494–1496 (2004)
- Zhang, J., Tian, J., Li, L.: A dual-band tunable metamaterial near-unity absorber composed of periodic cross and disk graphene arrays. *IEEE Photon. J.* **10**(2), 1–12 (2018)
- Zhu, J., Ma, Z., Sun, W., Ding, F., He, Q., Zhou, L., Ma, Y.: Ultra-broadband terahertz metamaterial absorber. *Appl. Phys. Lett.* **105**, 021102 (2014)